Supplements for
Modeling the evolution of the Structural Anisotropy of Snow

S. Leinss et al.

Correspondence: S. Leinss (leinss@ifu.baug.ethz.ch)

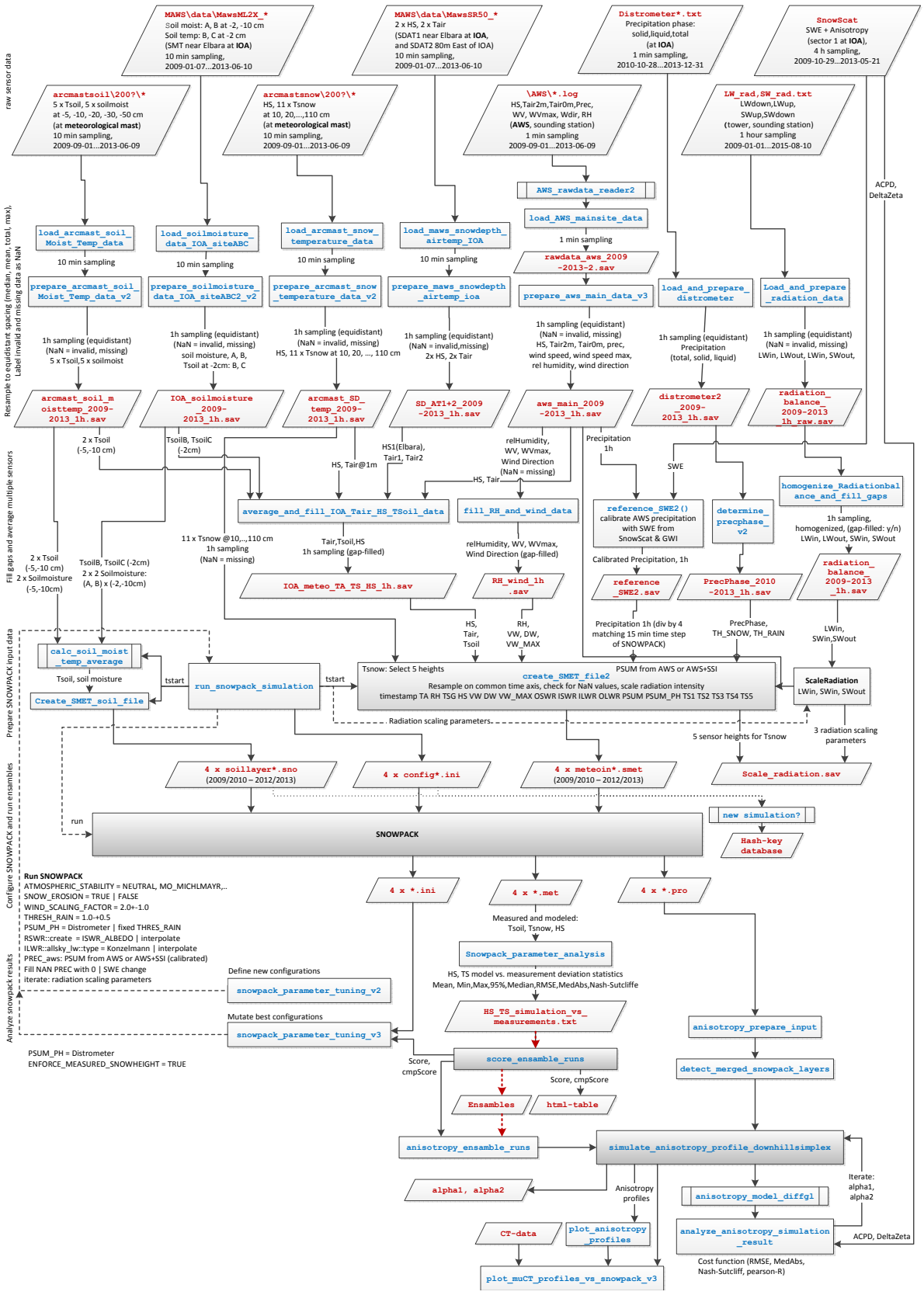

Figure 1. The flowchart presents the entire data flow for preprocessing of the meteorological data, configuration of snow pack, automated analysis and selection of SNOWPACK results, and finally the calibration and validation of our model.

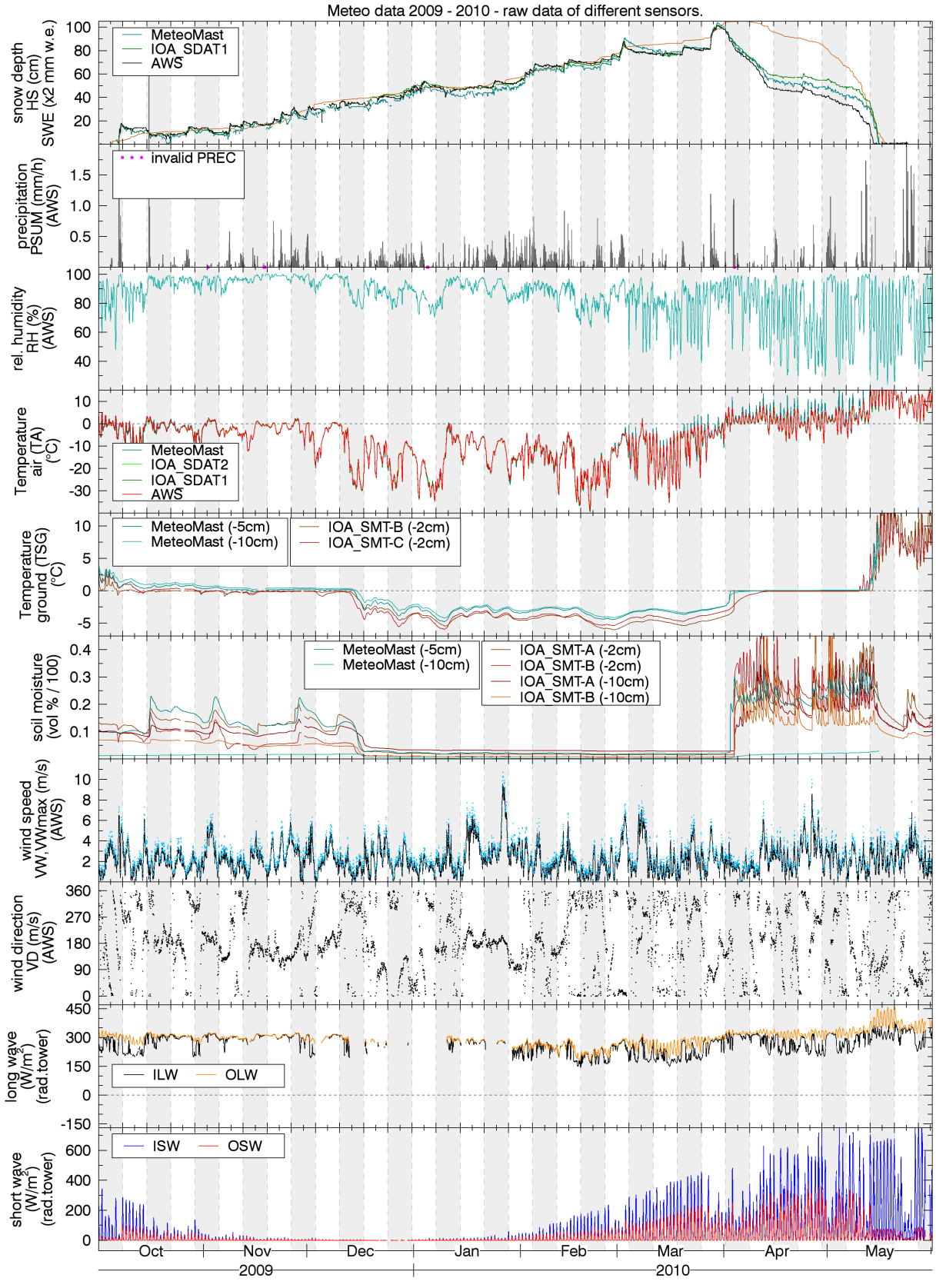

Figure 2. Raw meteodata 2009/2010 measured by different sensors.

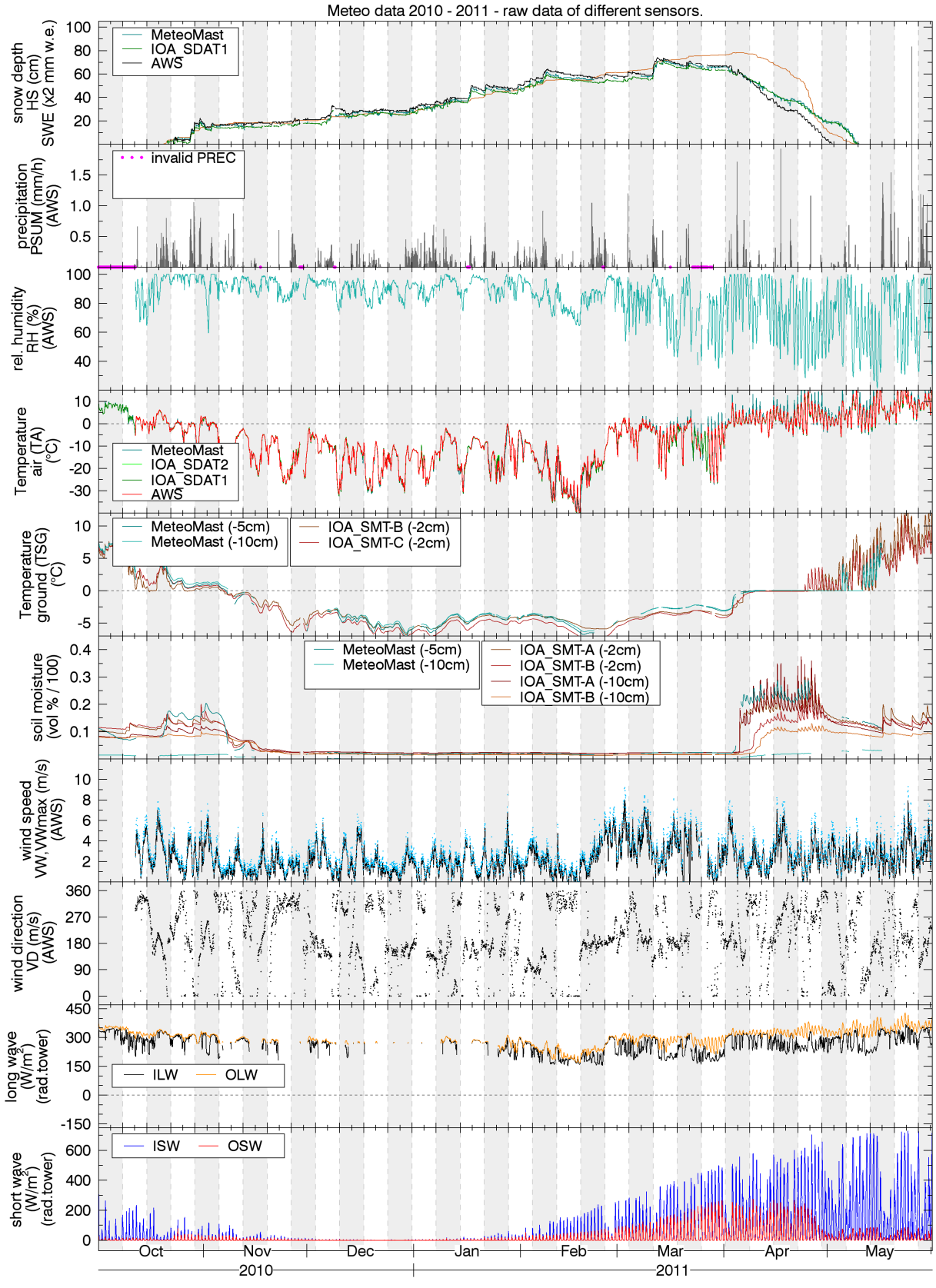

Figure 3. Raw meteodata 2010/2011 measured by different sensors.

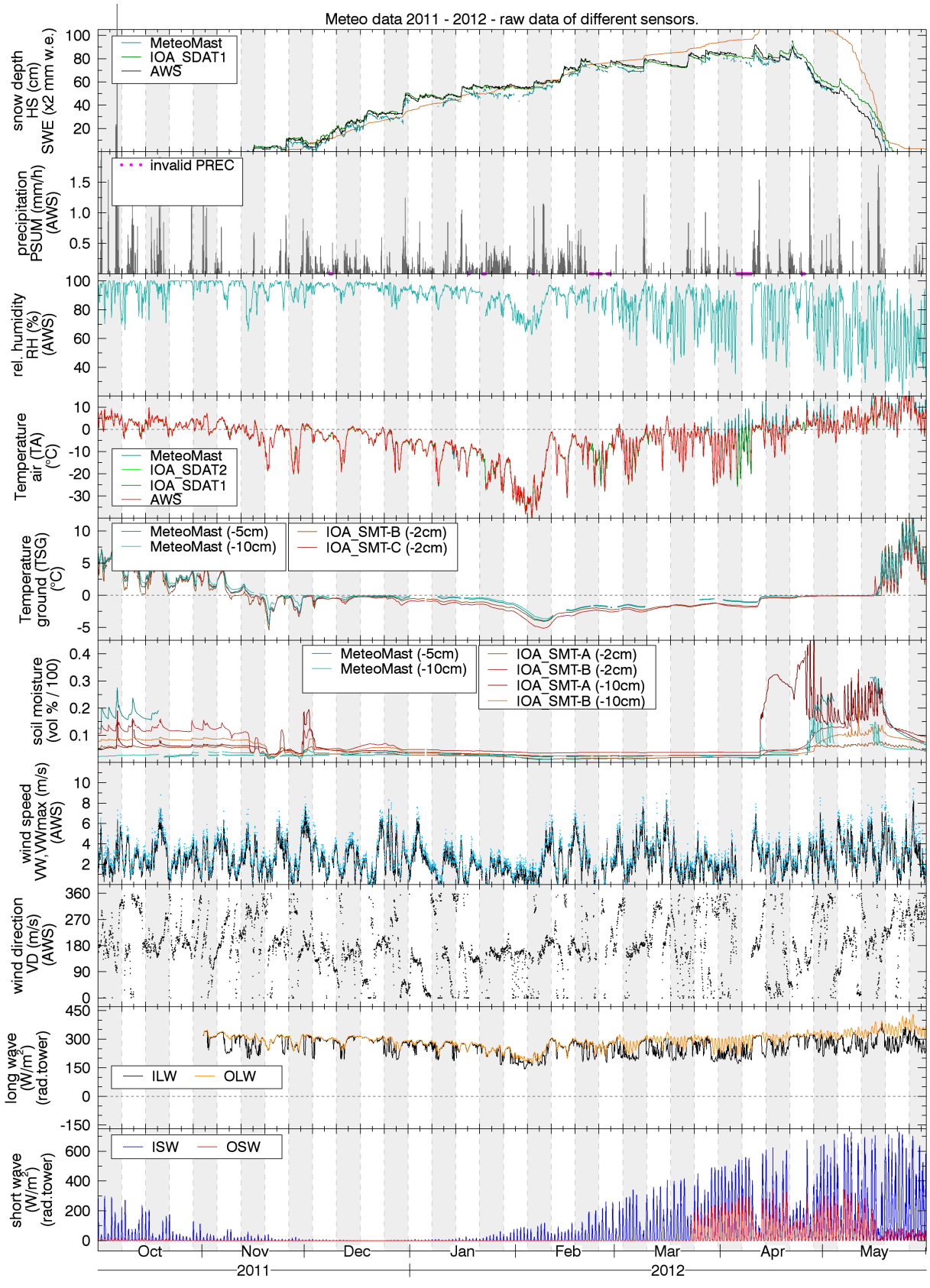

Figure 4. Raw meteodata 2011/2012 measured by different sensors.

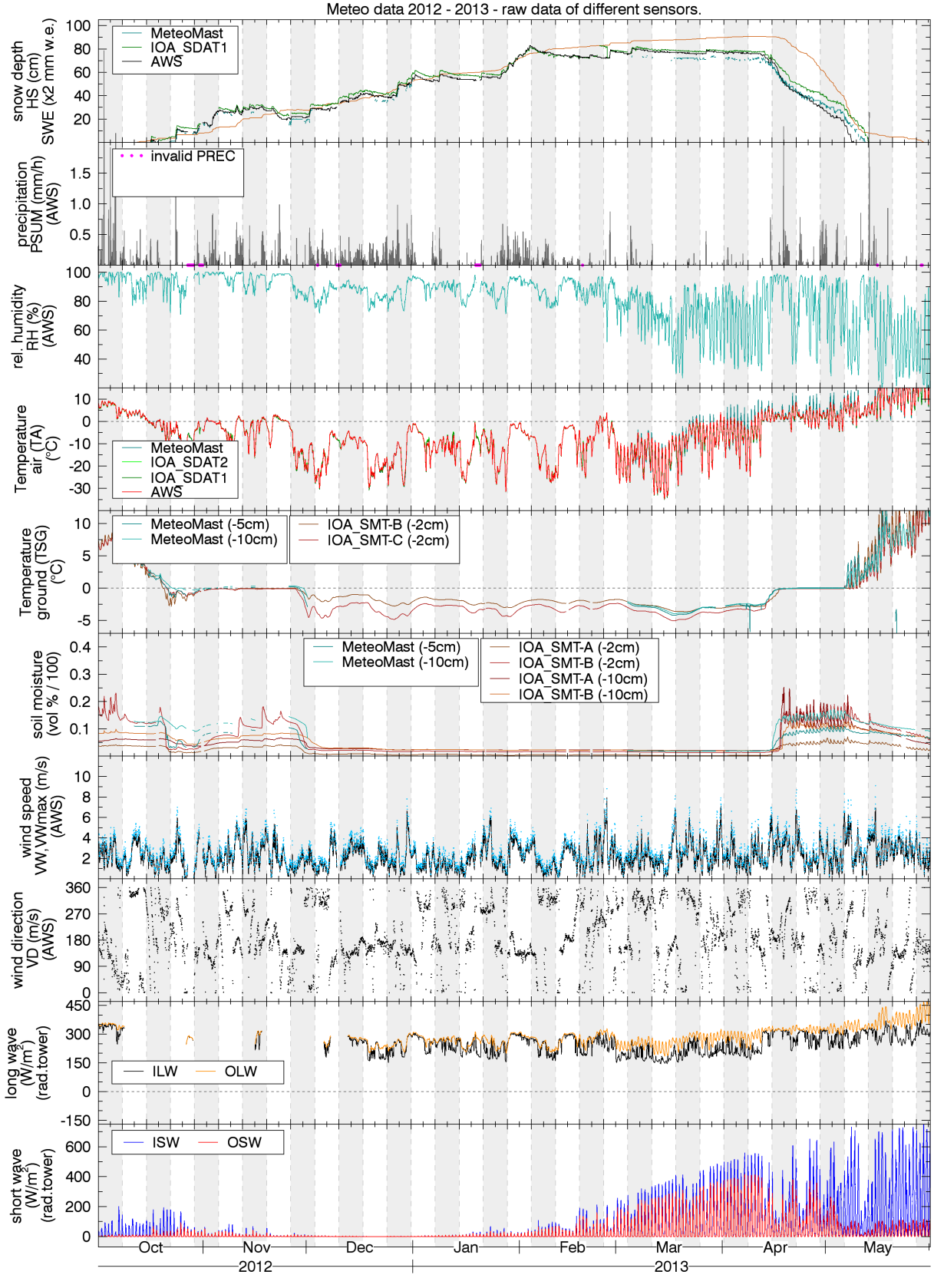

Figure 5. Raw meteodata 2012/2013 measured by different sensors.

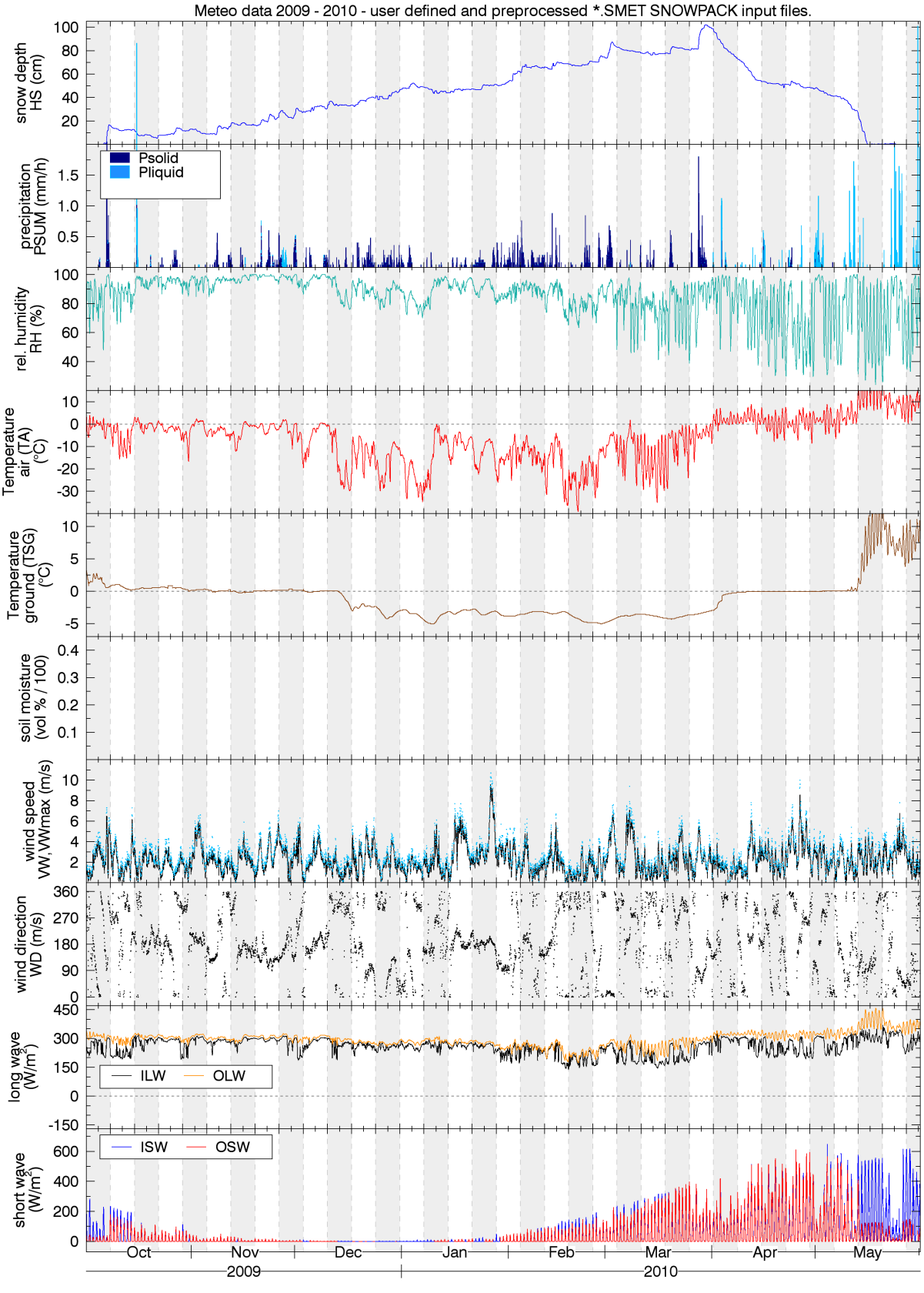

Figure 6. Meteodata 2009/2010 provided as SNOWPACK input (*.SMET files). (ensemble ID: optimizeradiation2458414-22890)

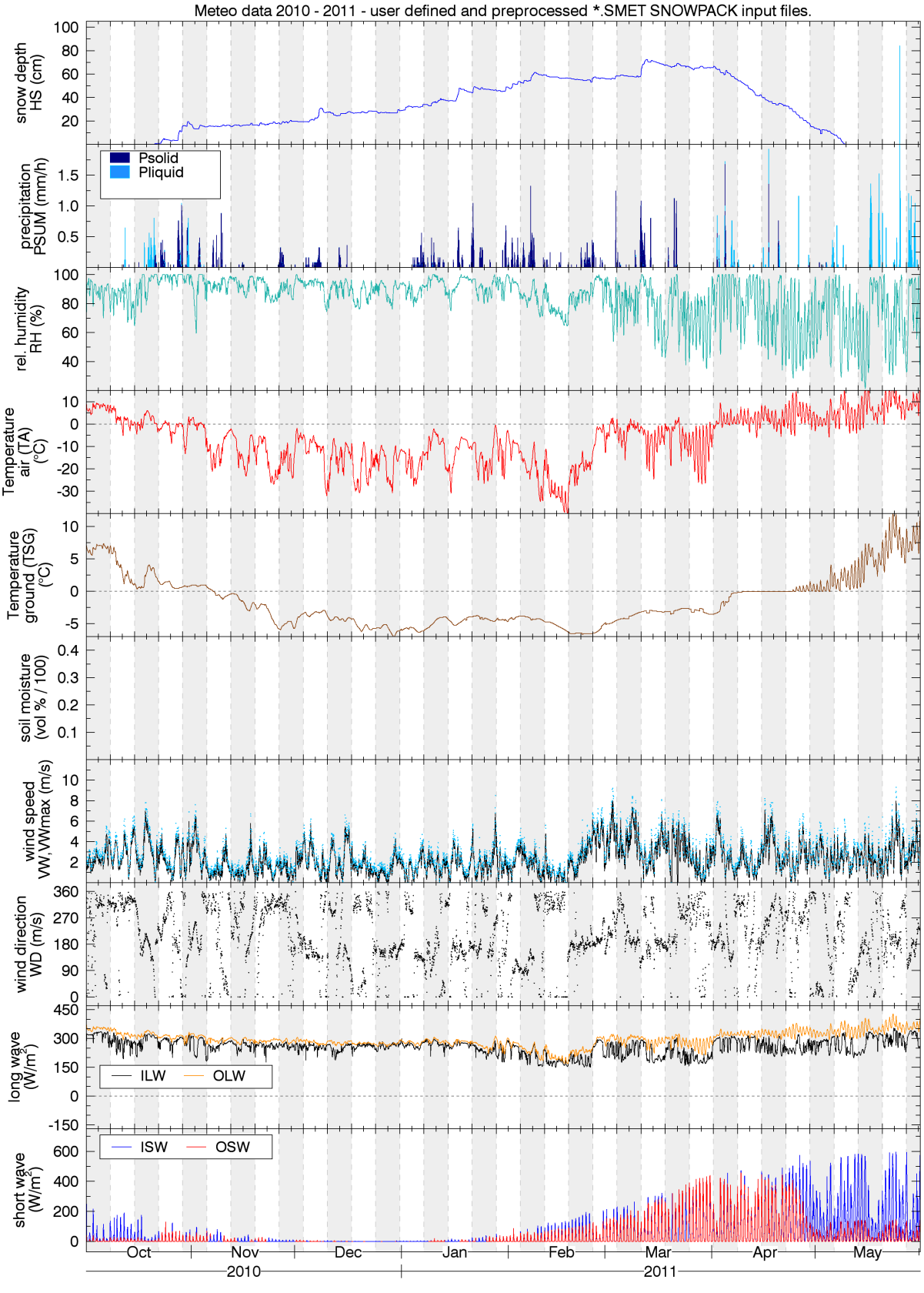

Figure 7. Meteodata 2010/2011 provided as SNOWPACK input (*.SMET files). (ensemble ID: optimizeradiation2458414-22890)

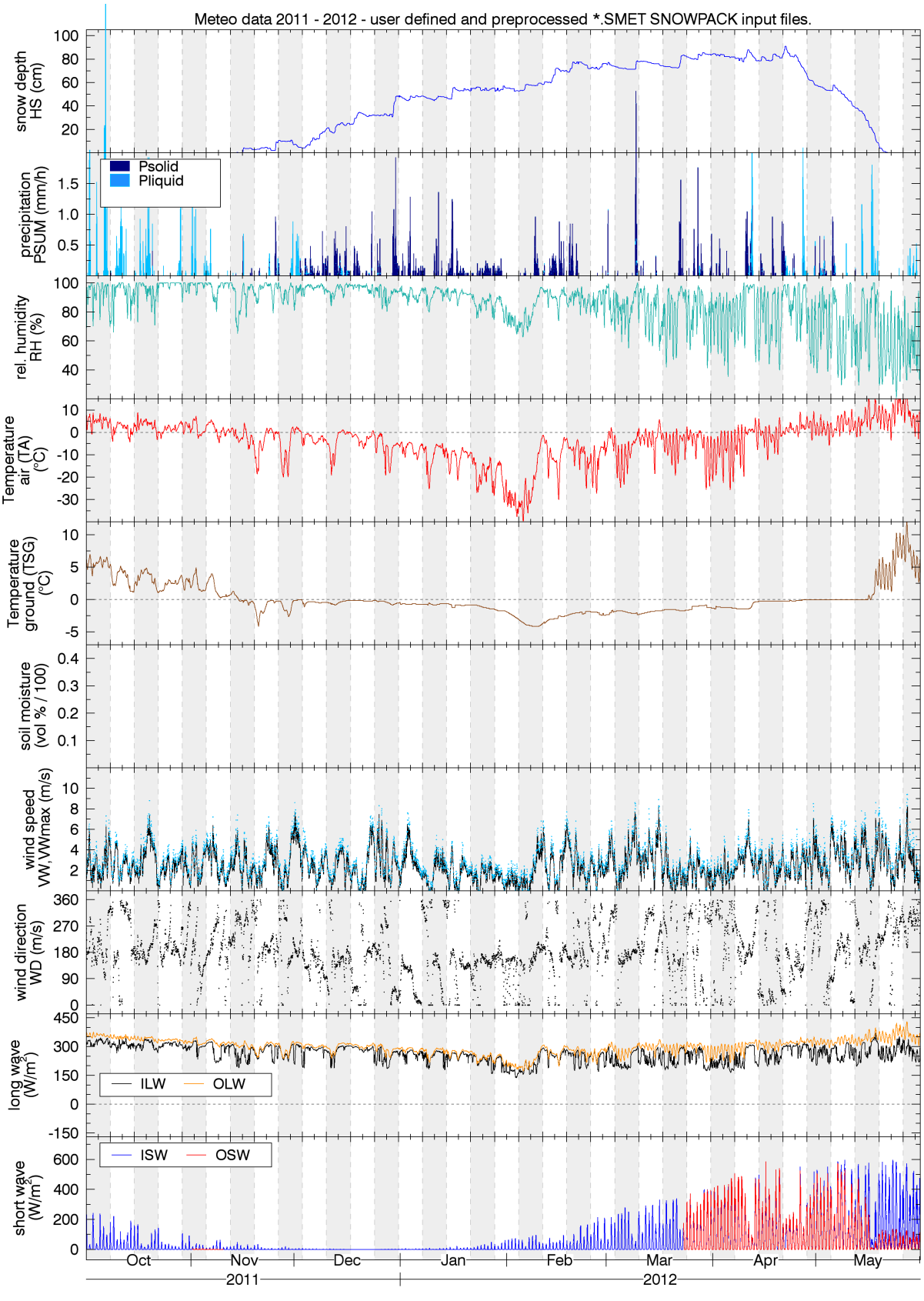

Figure 8. Meteodata 2011/2012 provided as SNOWPACK input (*.SMET files). (ensemble ID: optimizeradiation2458414-22890)

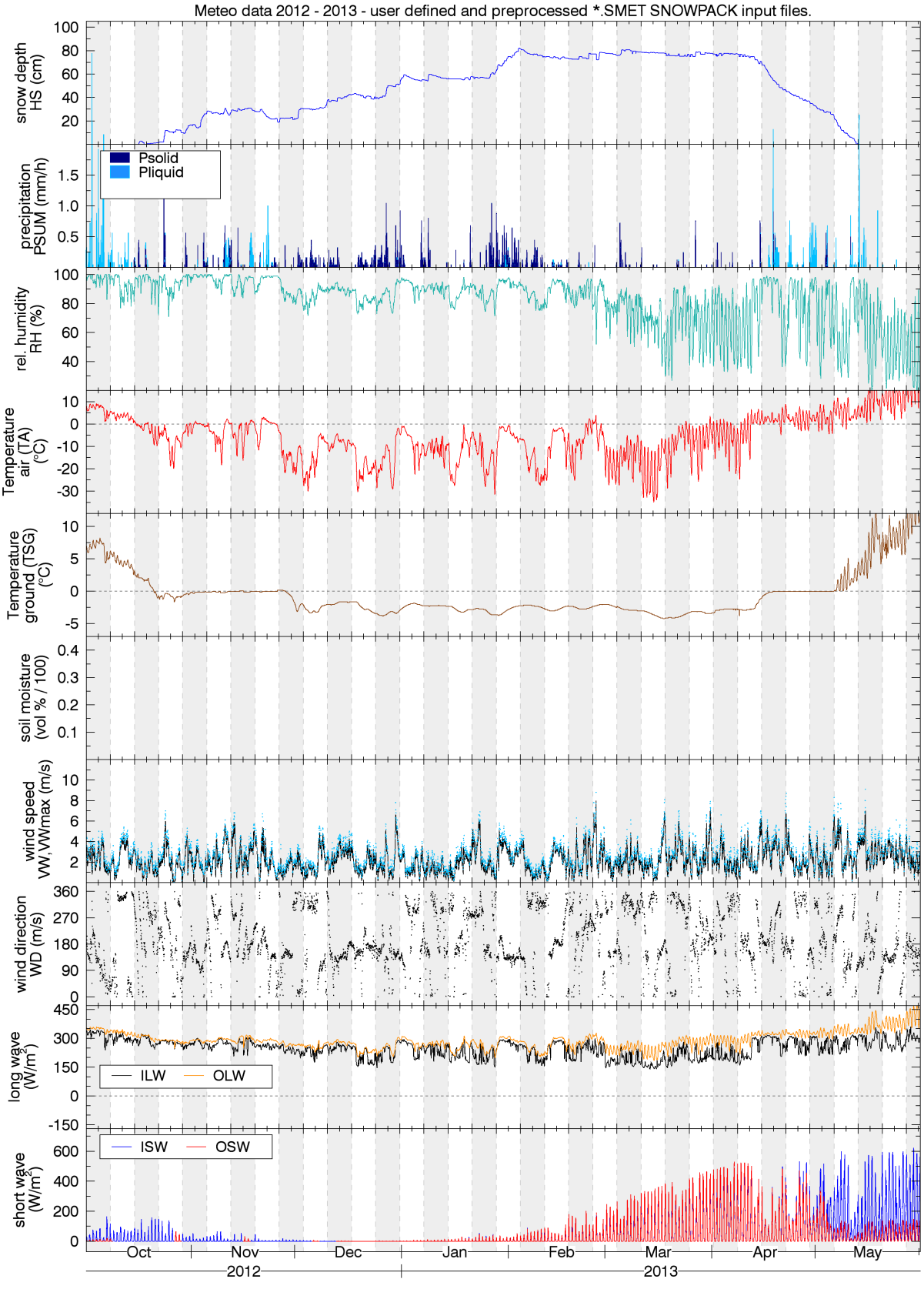

Figure 9. Meteodata 2012/2013 provided as SNOWPACK input (*.SMET files). (ensemble ID: optimizeradiation2458414-22890)

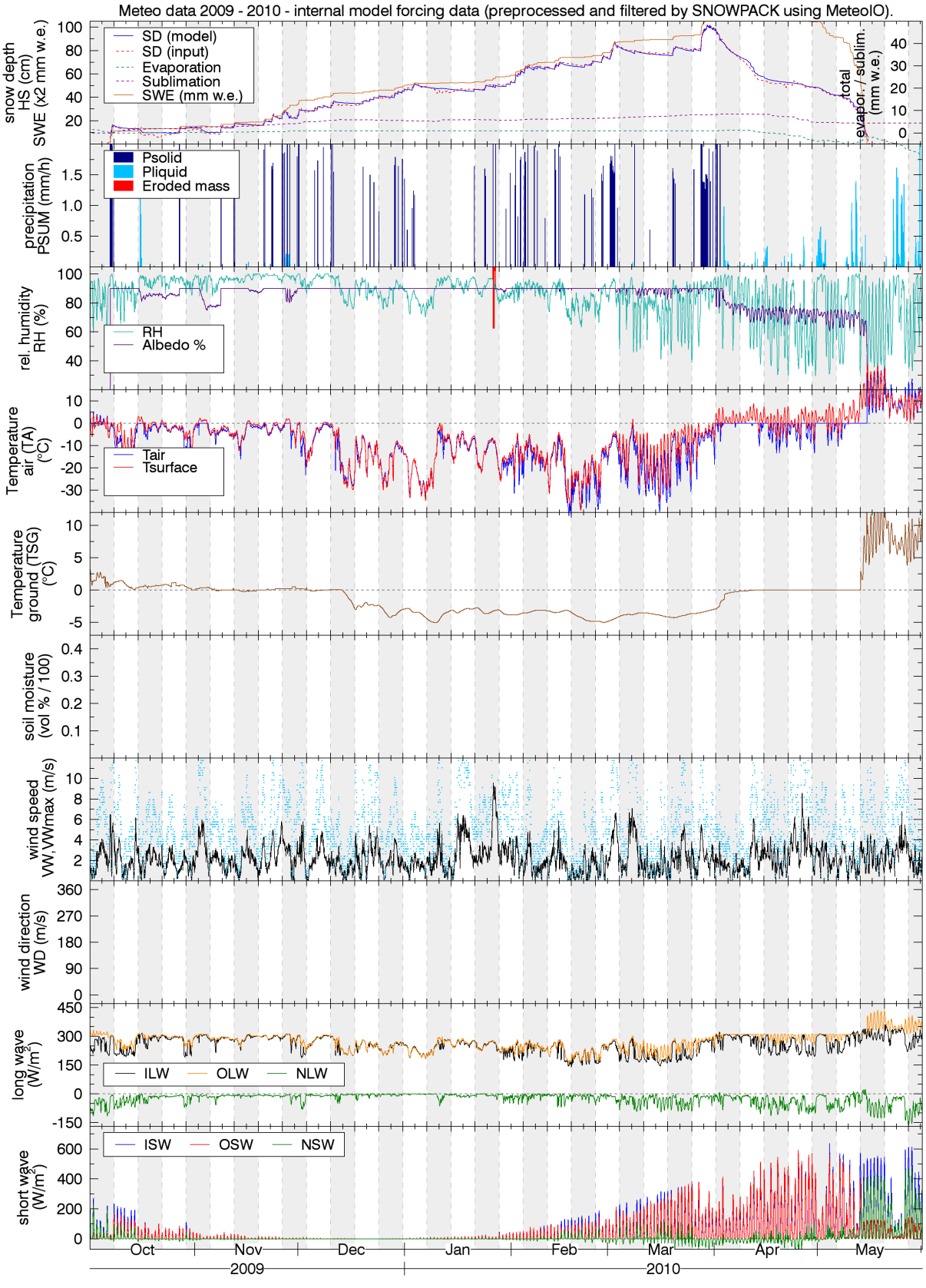

Figure 10. Meteodata 2009/2010, processed and filtered by SNOWPACK/MeteoIO. This data is the forcing data in the core of the model and is written out to *.met files (WRITE_PROCESSED_METEO = TRUE). HS was enforced (ensemble ID: optimizeradiation2458414-22890).

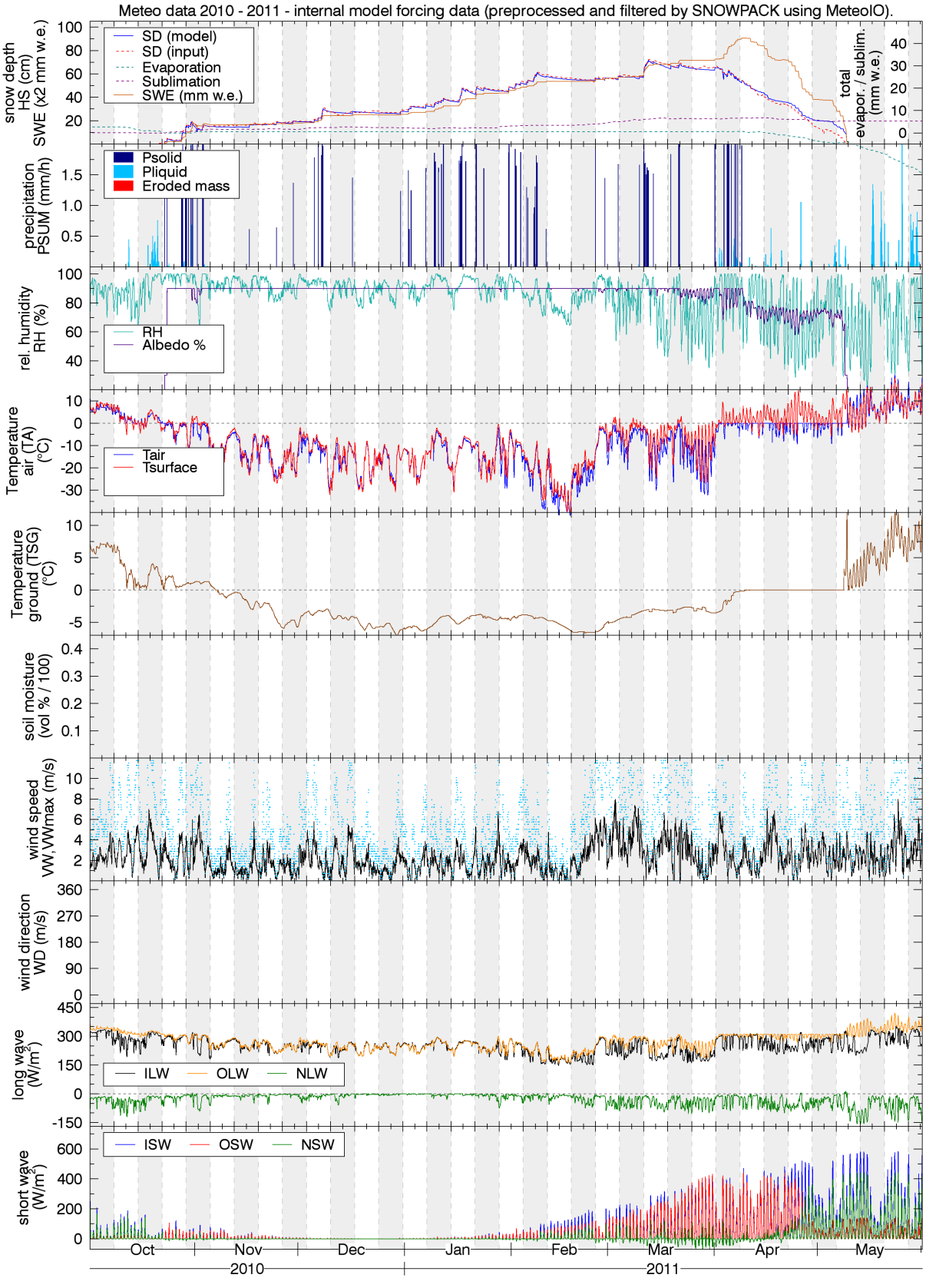

Figure 11. Meteodata 2010/2011, processed and filtered by SNOWPACK/MeteoIO. This data is the forcing data in the core of the model and is written out to *.met files (WRITE_PROCESSED_METEO = TRUE). HS was enforced (ensemble ID: optimizeradiation2458414-22890).

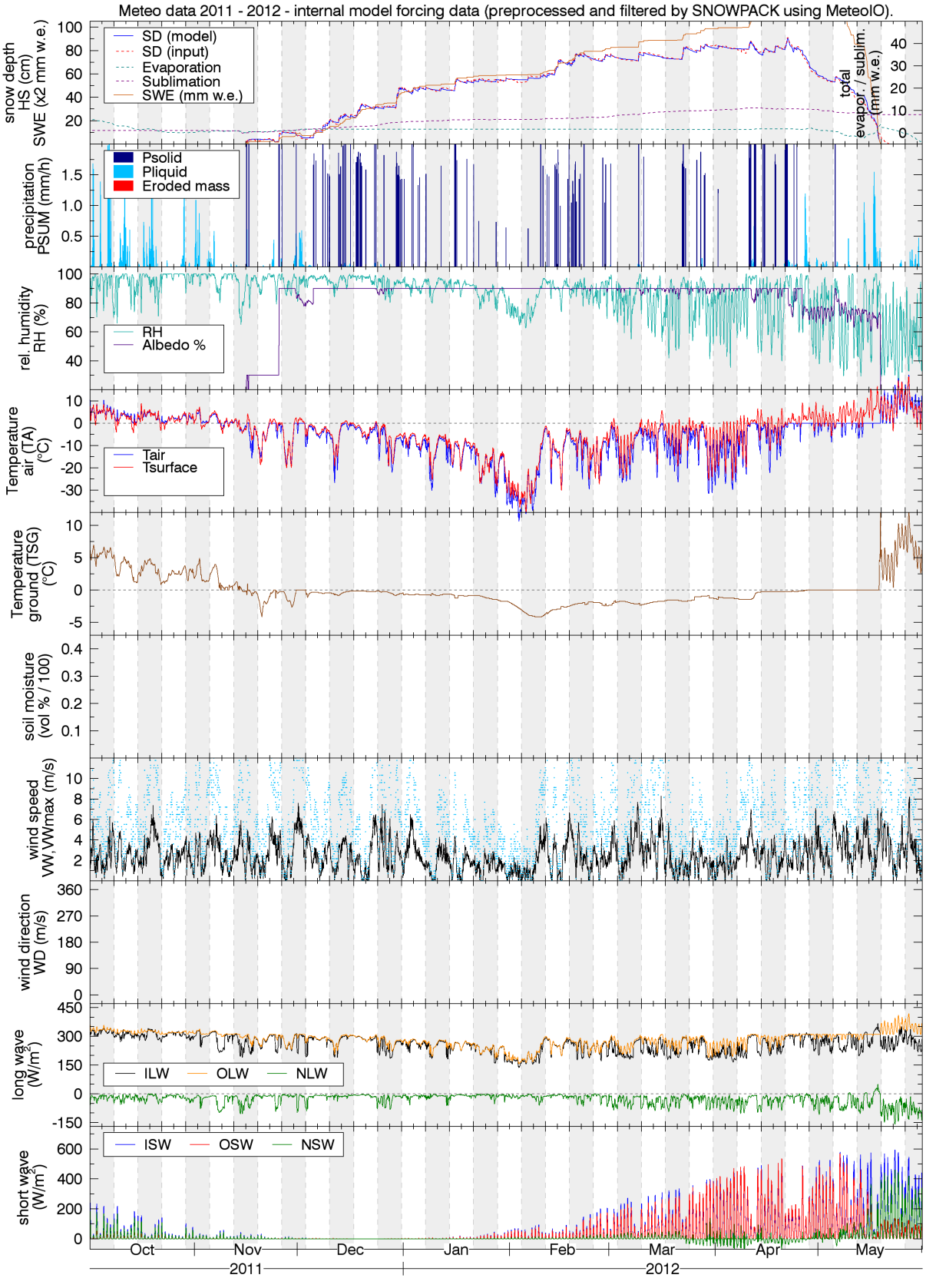

Figure 12. Meteodata 2011/2012, processed and filtered by SNOWPACK/MeteoIO. This data is the forcing data in the core of the model and is written out to *.met files (WRITE_PROCESSED_METEO = TRUE). HS was enforced (ensemble ID: optimizeradiation2458414-22890).

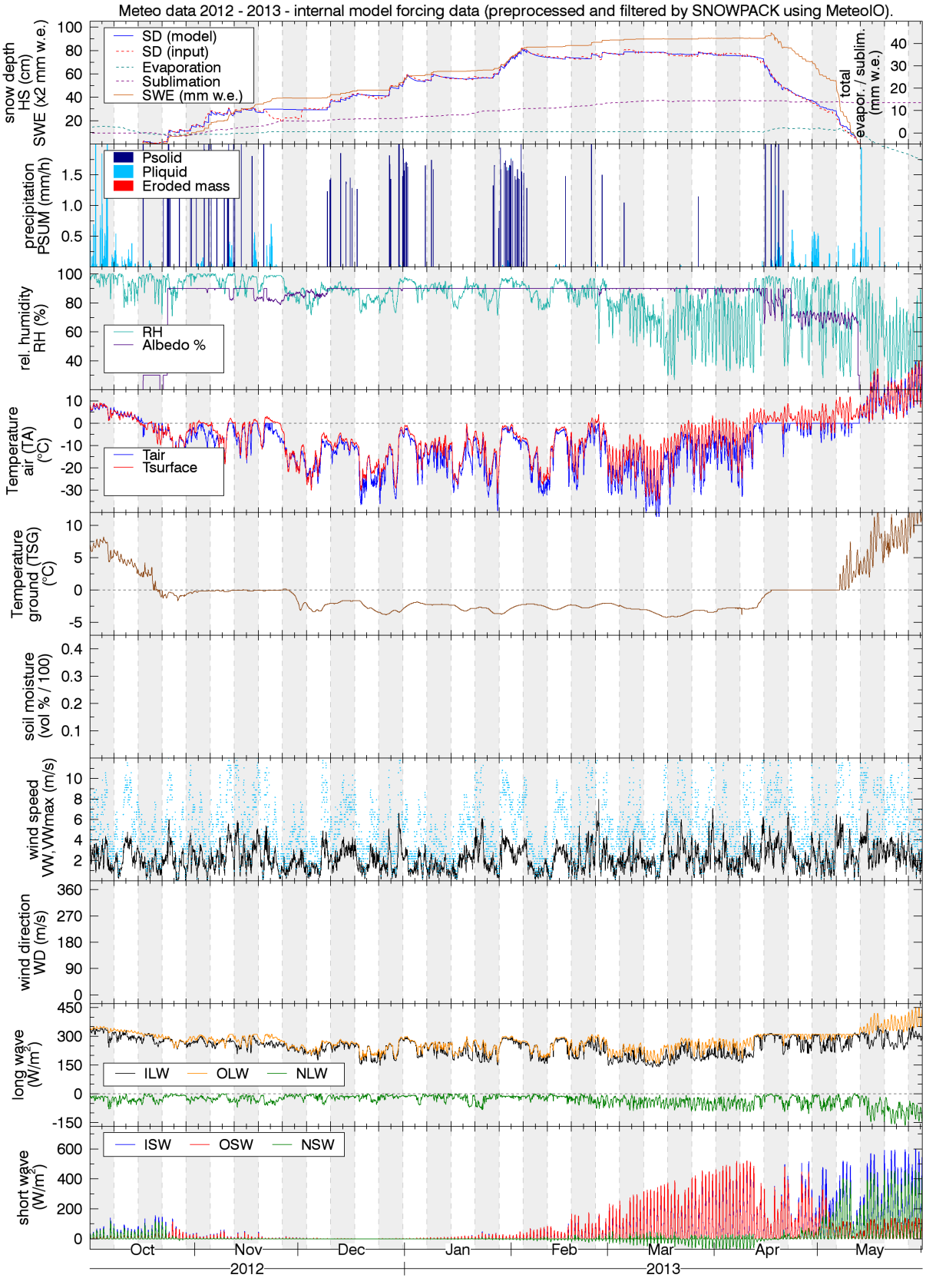

Figure 13. Meteodata 2012/2013, processed and filtered by SNOWPACK/MeteoIO. This data is the forcing data in the core of the model and is written out to *.met files (WRITE_PROCESSED_METEO = TRUE). HS was enforced (ensemble ID: optimizeradiation2458414-22890).

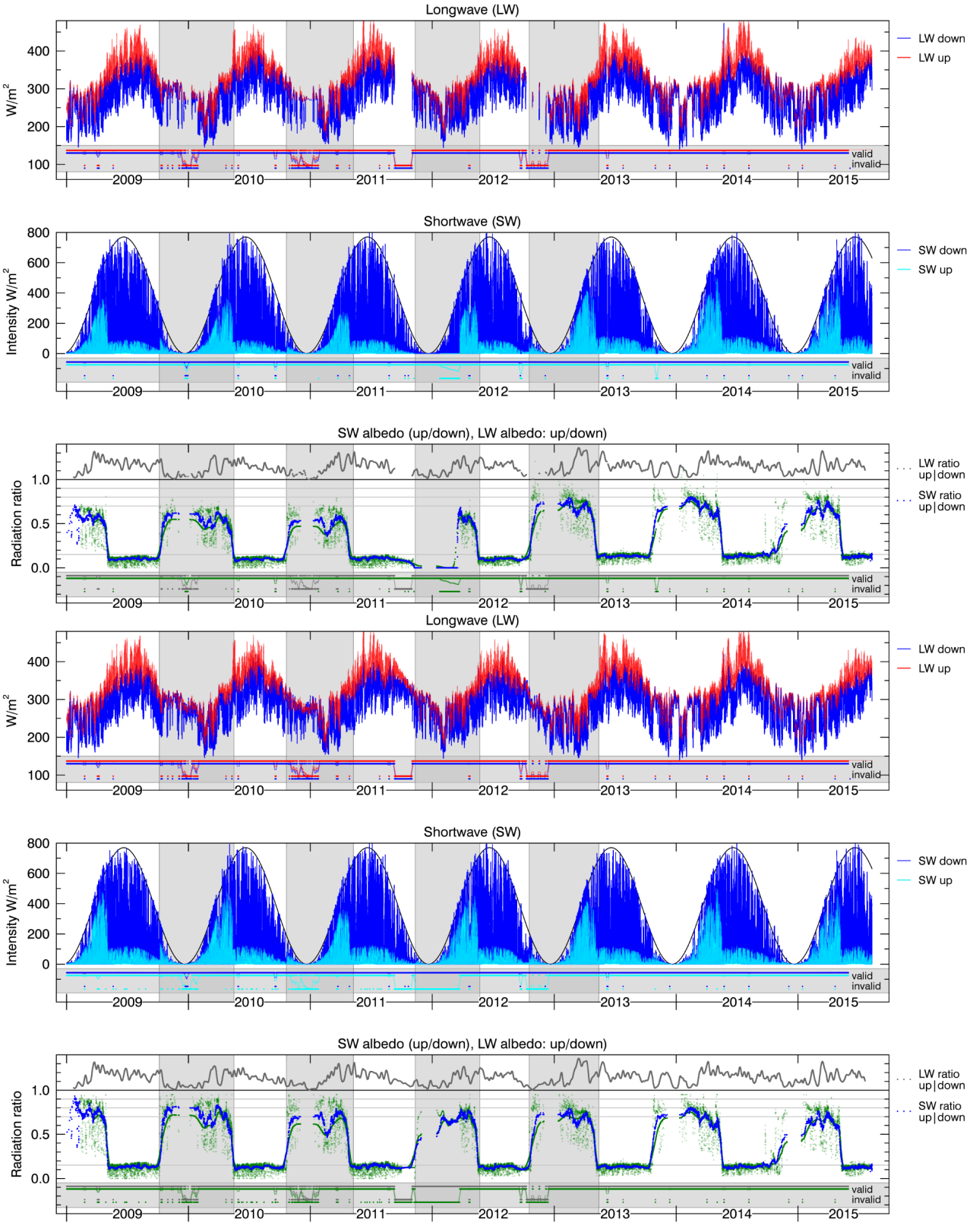

Figure 14. Top three graphs: raw radiation data, gaps show invalid or missing data. Bottom three graphs: filled and homogenized radiation data. The short wave sensor was replaced in August 2012.

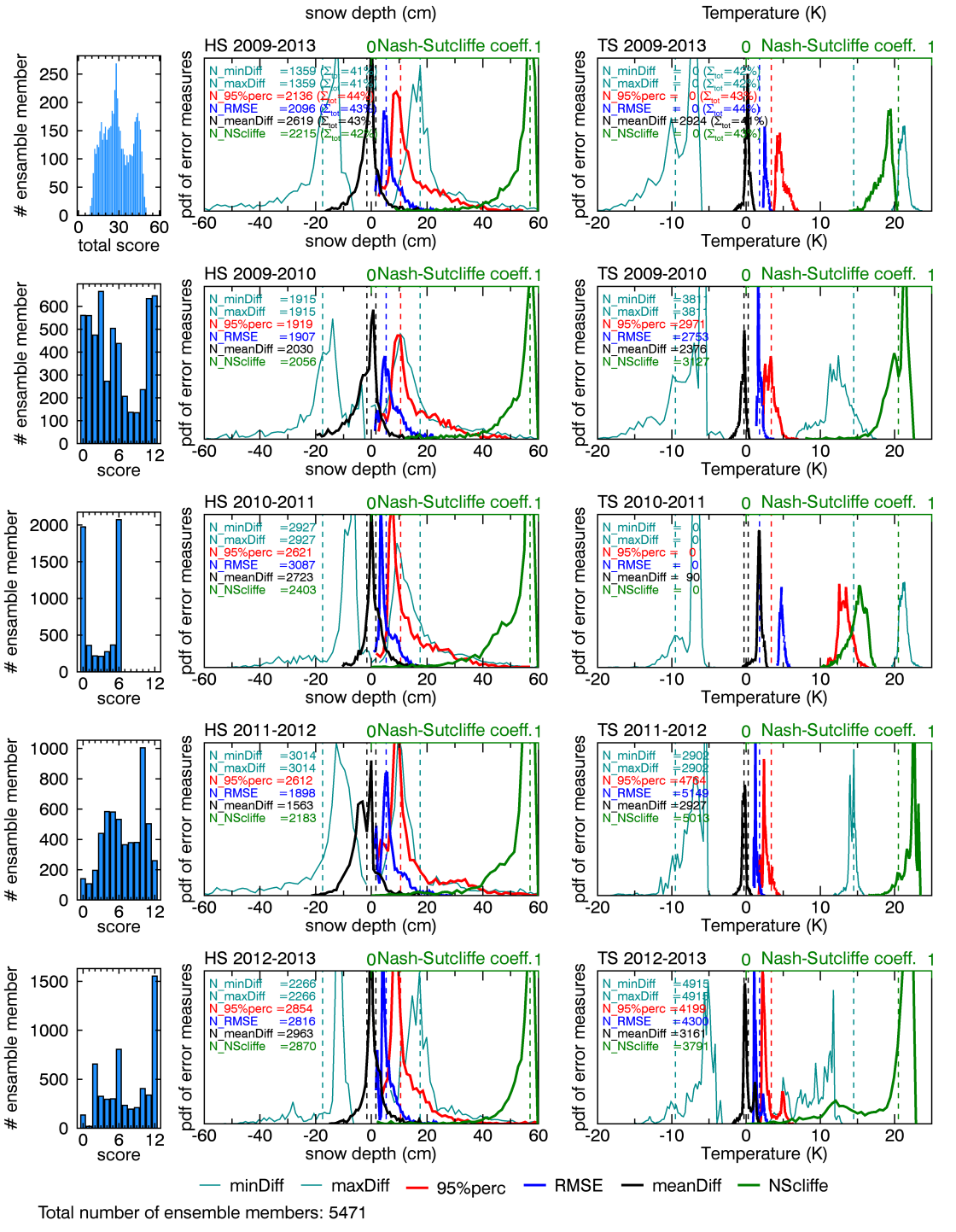

Figure 15. Histograms of the six statistical descriptors (see legend) used to measure the accuracy of different SNOWPACK runs. The descriptors rate the difference between measured and simulated values for snow height (HS) and snow temperature (TS). The shown histograms of the descriptors cover all SNOWPACK ensemble runs with different settings and radiation scaling parameters. The top row shows the statistics over all four seasons; the lower four rows are the statistic for each individual season. The left column shows the score of each season and the total score determined by thresholding. The thresholds are shown as vertical dashed lines. Numerical values of the thresholds are given in the main document.

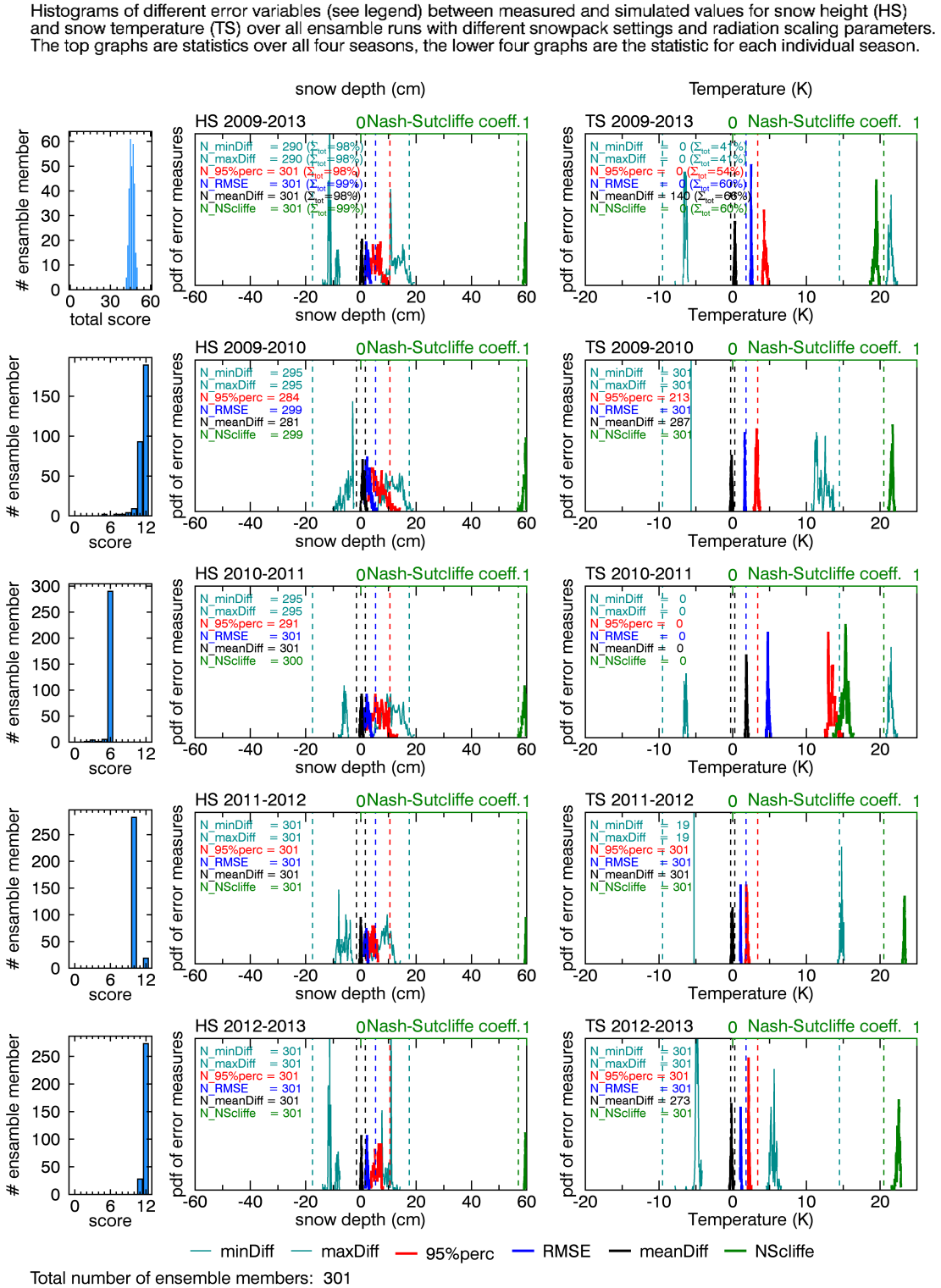

Figure 16. Histograms of the six statistical descriptors (see legend) for the best 301 snow pack runs. The descriptors rate the difference between measured and simulated values for snow height (HS) and snow temperature (TS). The shown histograms of the descriptors cover all SNOWPACK ensemble runs with different settings and radiation scaling parameters. The top row shows the statistics over all four seasons; the lower four rows are the statistic for each individual season. The left column shows the score of each season and the total score determined by thresholding. The thresholds are shown as vertical dashed lines. Numerical values of the thresholds are given in the main document.

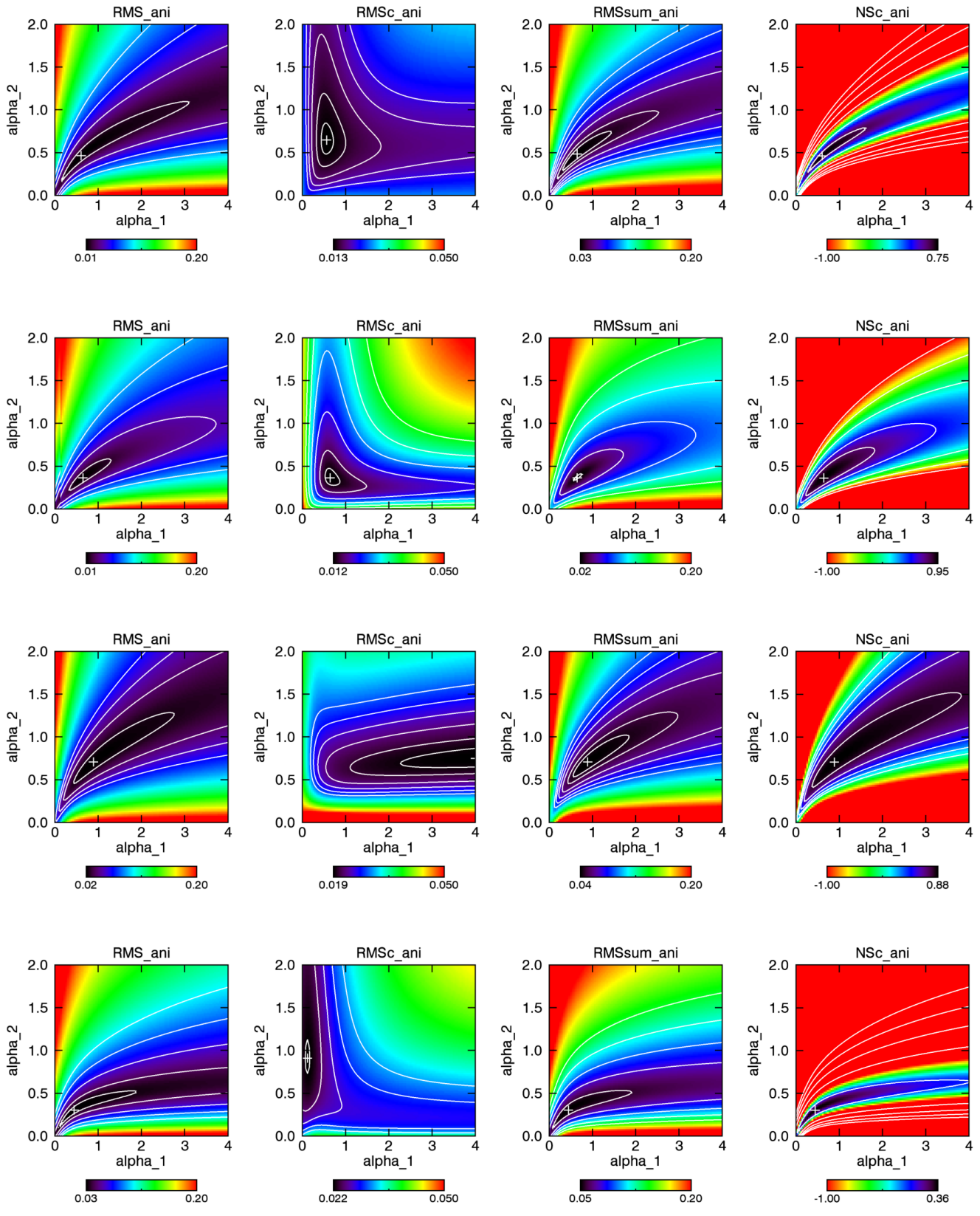

Figure 17. Cost functions for individual seasons. Each line represents the cost function for an individual season (2009/2010–2012/2013). Each column shows the cost function for (1): only the first term of the cost function; (2): only the second term of the cost function, (3): the sum of the first and second term; (4): The Nash-Suttcliffe model efficiency coefficient.

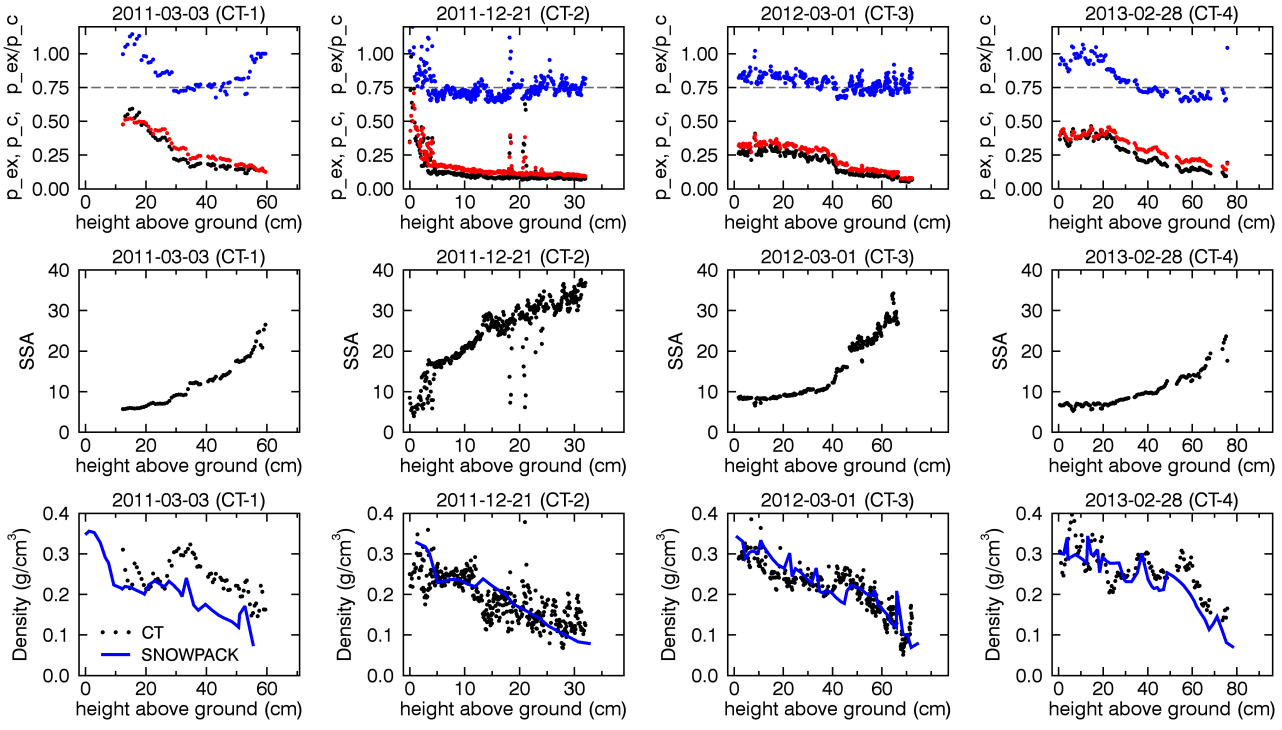

Figure 18. Further parameters derived from the CT data. Top row: exponential correlation length (p_{ex}, black), slope of the correlation function at the origin (p_{c}, red) and the ratio $p_{\mathrm{ex}}/p_{\mathrm{c}}$. The dashed lines indicates the commonly used ratio $p_{\mathrm{ex}}/p_{\mathrm{c}} \approx 0.75$ which is not valid for depth hoar (Mätzler, 2002). Middle row: SSA, bottom row: density from CT data compared with density of the SNOWPACK simulation with enforced snow height (ID: optimizeradiation2458414-22890).

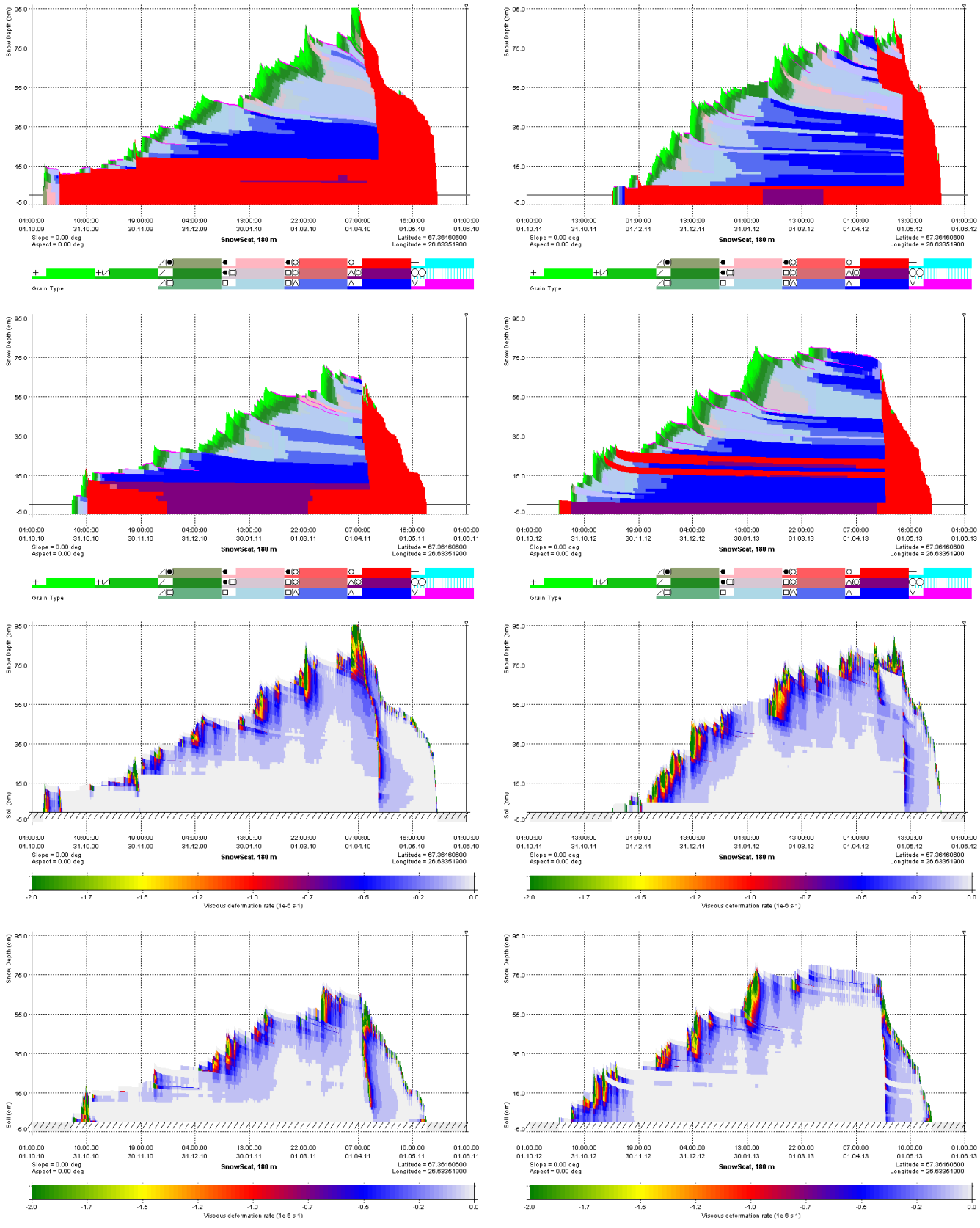

Figure 19. SNOWPACK visualizations for grain type classification and viscous deformation rate.

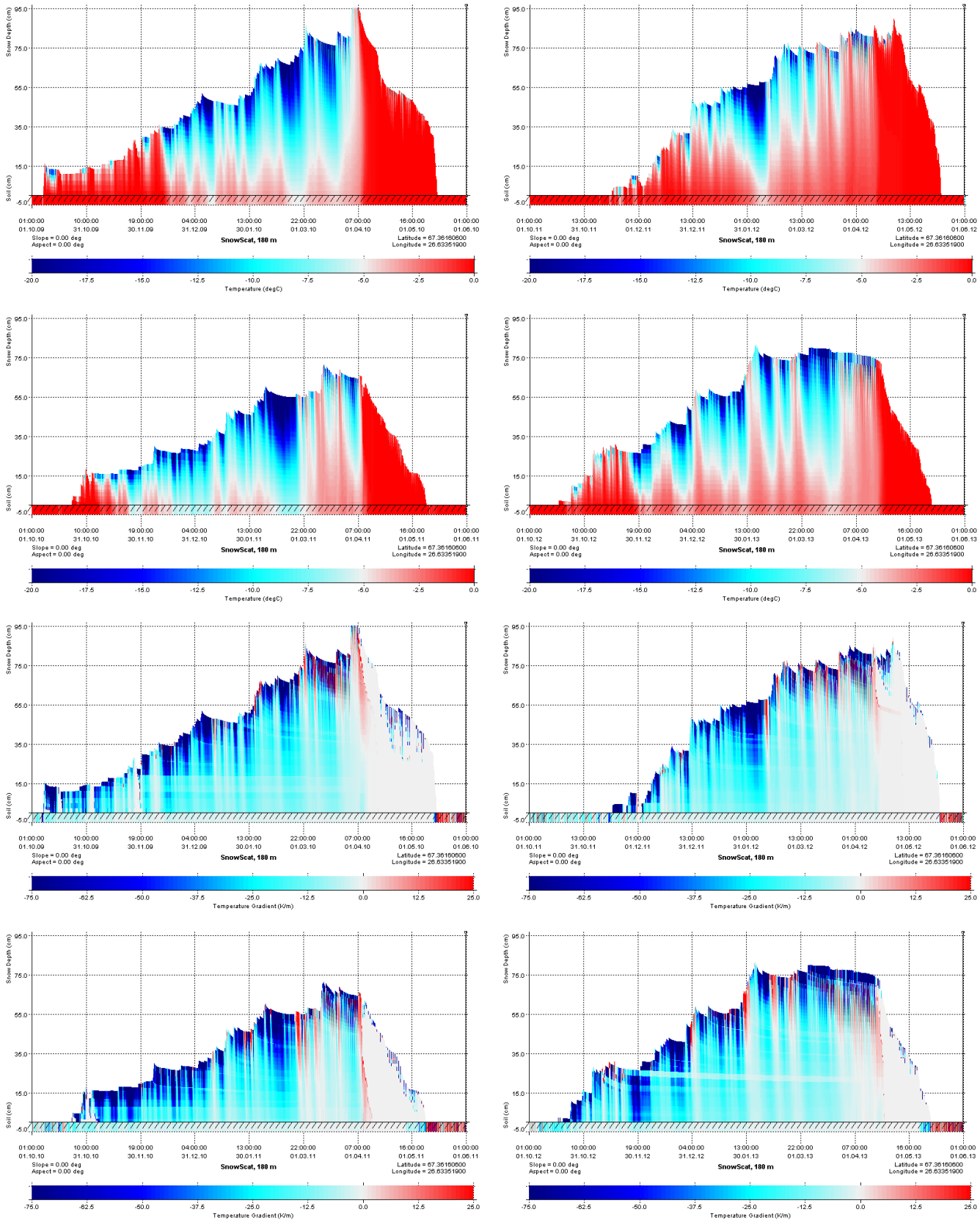

Figure 20. SNOWPACK visualizations for snow temperature and temperature gradient.

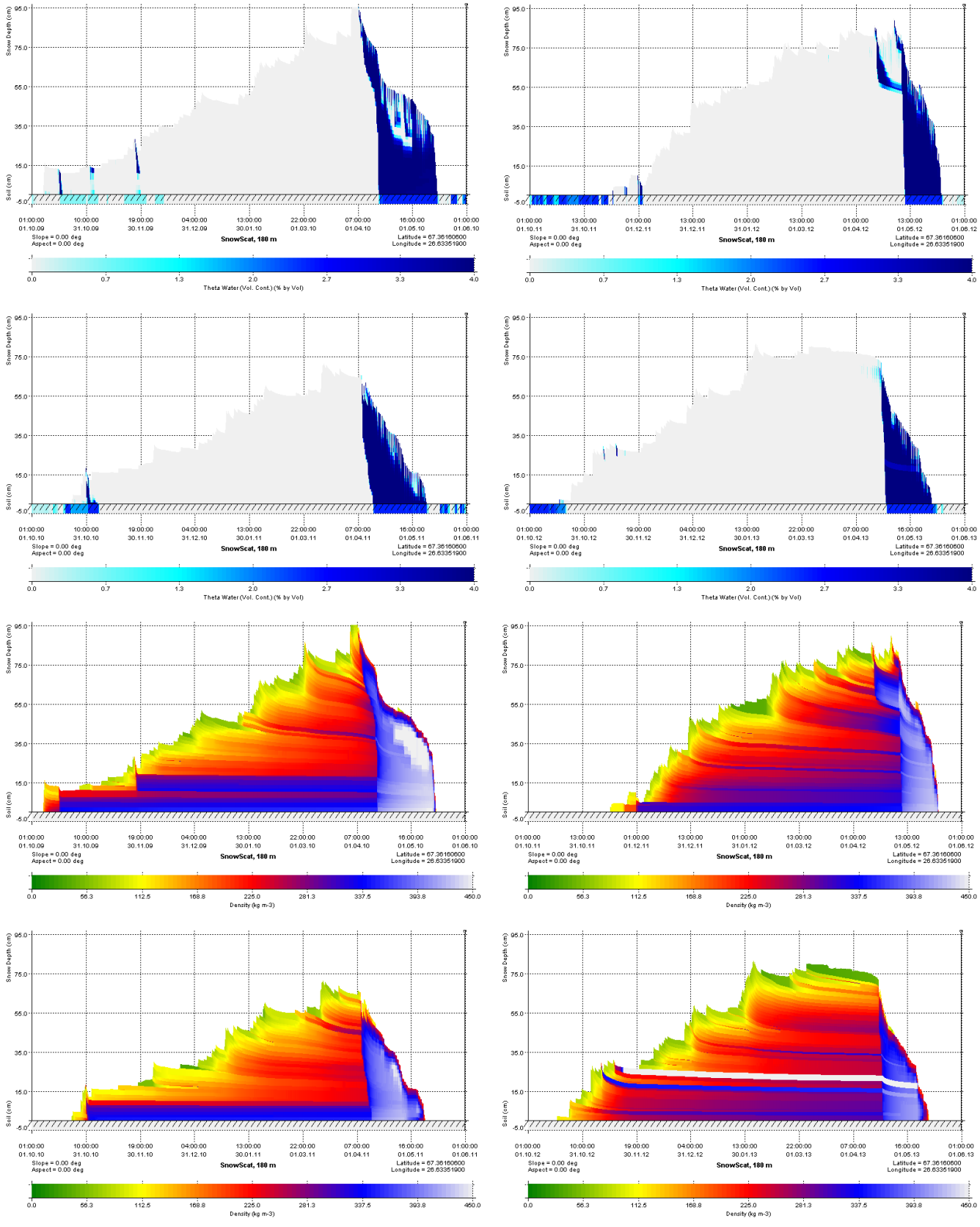

Figure 21. SNOWPACK visualizations for liquid water fraction and snow density.

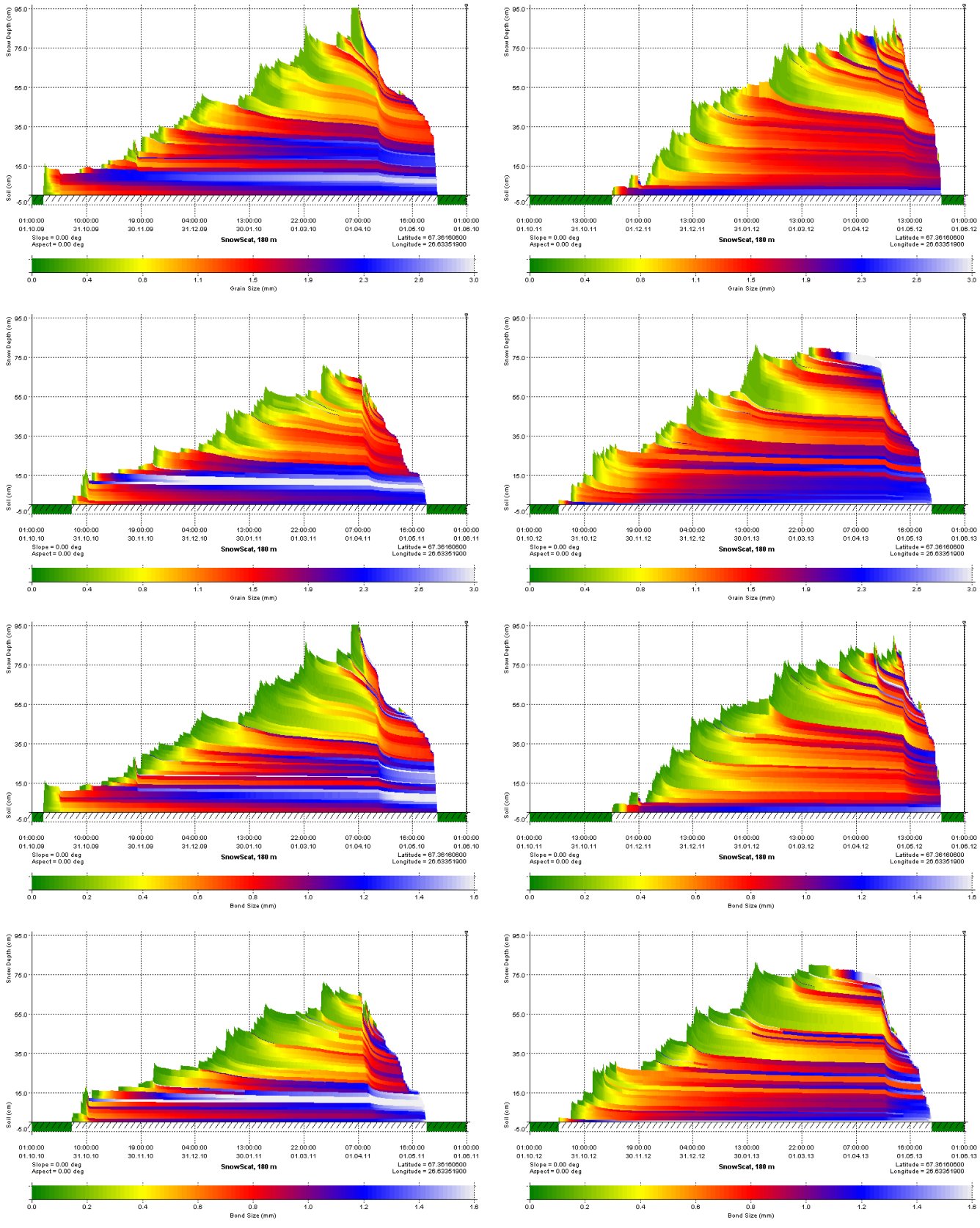

Figure 22. SNOWPACK visualizations for grain size and bond size.

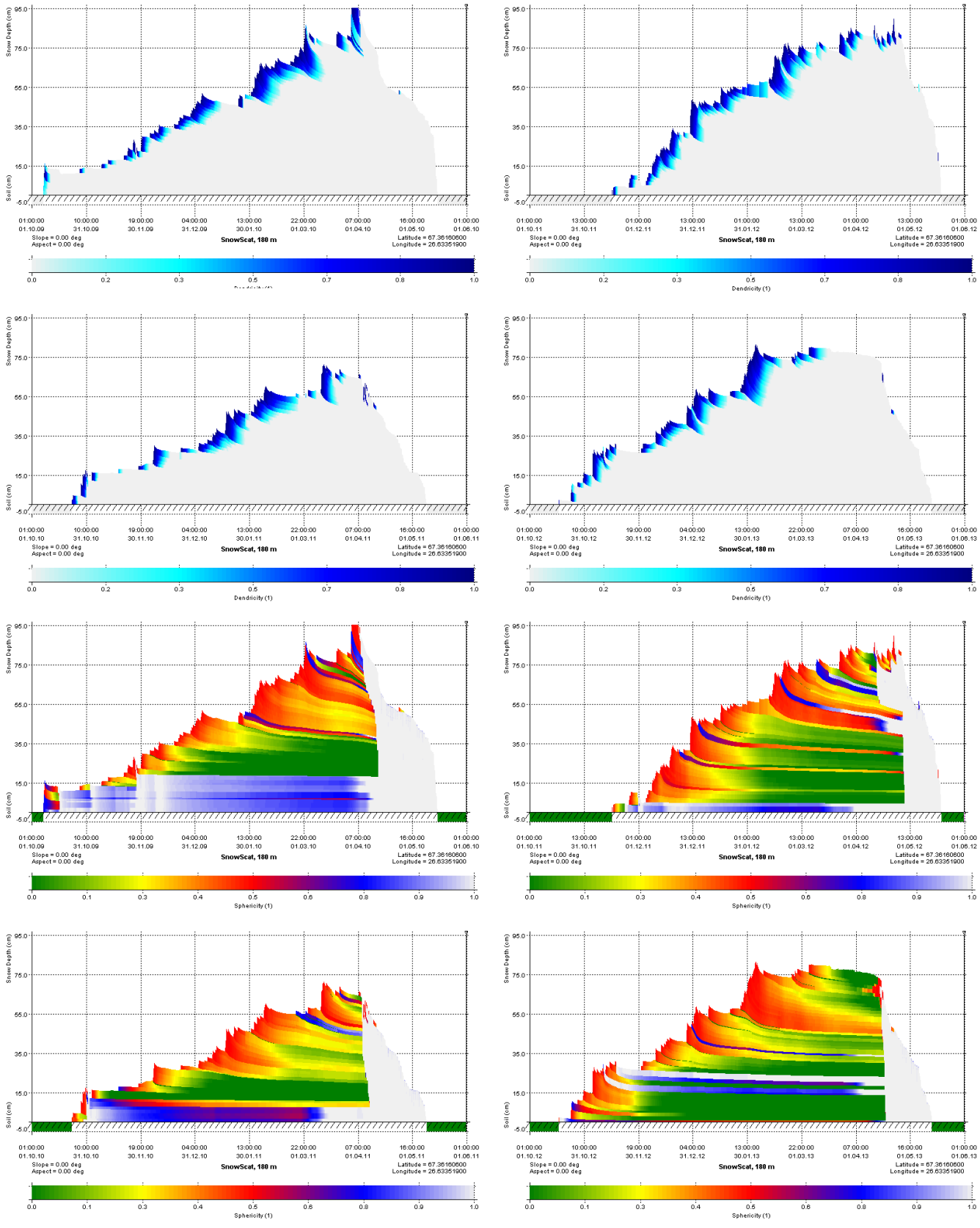

Figure 23. SNOWPACK visualizations for dentricity and sphericity.

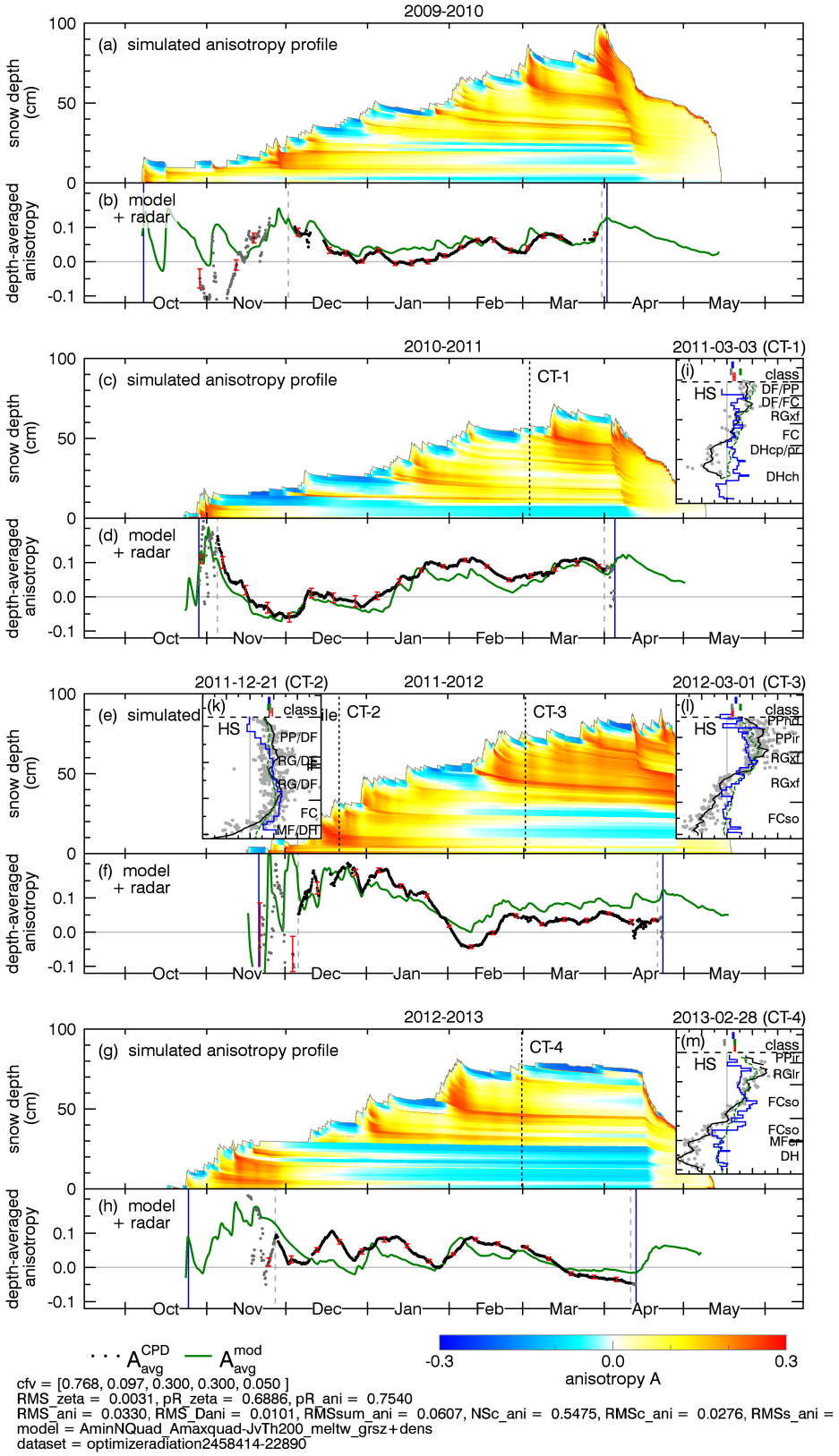

Figure 24. Modeled solution when grain size is considered by setting the microstructural term $f_\mu = \rho_{\text{snow}} r_g$.